SUPER-HARMONIC VIBRATIONS OF MODEL-SCALE RISER PIPES

R.J. McSherry, J.M.R. Graham
Department of Aeronautics, Imperial College London, U.K.
R.H.J. Willden
Department of Engineering Science, University of Oxford, U.K.

ABSTRACT

Presented in this paper are the results of numerical simulations of the Vortex-Induced Vibrations of a model scale marine riser pipe. The investigation has its genesis in a direct comparison between the predictions of a coupled strip theory Computational Fluid Dynamics code and the long model riser experiments that were commissioned by the Norwegian Deepwater Programme and performed by Marintek in the Trondheim Ocean Basin in 2003. The riser had a length-to-diameter ratio of approximately 1400 and was subjected to uniform and linearly sheared flows in the sub-critical Reynolds number regime. Numerical predictions of the riser vibrations for these two flow profiles are found to agree well with experimental findings. Of particular interest is the occurrence in the simulations of harmonic responses at multiples of the principal cross-flow and in-line oscillation frequencies, which in some cases are found to be dominant with respect to riser curvature. The investigation has been expanded to include less idealised flow profiles; there are strong early indications that it is possible for harmonic responses to be dominant with respect to curvature in realistic uni-directional flows.

1. INTRODUCTION

Growing research attention is being paid to the occurrence of harmonically-excited modes of vibration in long marine riser pipes. It is thought that these higher harmonic responses can, in some circumstances, dominate the pipe's curvature variation along its length, which in turn can lead to an increase in the pipe's fatigue damage rate. The present study is motivated by the need to better understand and predict the Vortex-Induced Vibrations (VIV) of marine riser pipes, and in particular the desire to assess the extent to which harmonic excitation can influence fatigue life in realistic flow profiles.

The paper presents a numerical investigation of the VIV of a tension-dominated model riser of length-to-diameter ratio, L/D, of 1407. The numerical simulations replicate and extend the experimental investigation of Trim et al. (2005), in which a model riser was towed horizontally through still water at speeds that gave rise to Reynolds numbers in the range $7099 \leq Re \leq 56000$ (where $Re = UD/\nu$ is the Reynolds number and U, D and ν are the flow speed, cylinder diameter and kinematic viscosity respectively). Trim et al. investigated both uniform and linearly-sheared flow profiles. The model riser had low structural damping, 0.3% of critical, and its mass ratio, the ratio of its structural mass to the mass of fluid displaced by it, was 1.6. The simulations presented in this paper extend Trim et al.'s investigation by considering both profiles considered in their experiment, along with four additional flow profiles, including two more realistic profiles representative of typical profiles found in the Gulf of Mexico and the West of Shetland regions.

The numerical simulations are conducted using a strip theory Computational Fluid Dynamics (CFD) code, VIVIC (Willden, 2003), details of which are presented in the next section. Following this is a brief account of a rigorous benchmarking exercise, in which the flow solver was tested against high quality data from prescribed oscillation experiments performed at sub-critical Reynolds numbers. Following this are presented the results of the present riser VIV investigation.

2. NUMERICAL METHOD

VIVIC, which was developed at Imperial College London by Graham and Willden, is a strip theory CFD code in which the evolution of the flow is computed on multiple two-dimensional planes that are positioned at intervals along the axis of a long vibrating pipe. In each of these planes the flow evolution is computed by solving the velocity-vorticity formulation of the incompressible Navier-Stokes equations in two-dimensions. The correlating effect of lock-in (Toebes, 1969) is used to justify the assumption of local flow two-

dimensionality. The non-dimensional equation of fluid motion is given by:

$$\frac{\partial \omega}{\partial t} + (\mathbf{u}.\nabla)\omega = \frac{1}{Re}\nabla^2\omega \qquad (1)$$

where $\mathbf{u}$, ω and t are the non-dimensional velocity vector, spanwise component of vorticity and time. Non-dimensionalisation is based on the characteristic length and speed; D and U.

A first order time split approach is used to solve equation (1): the diffusion of vorticity is modelled using an Eulerian linear finite element approach across an unstructured triangular element mesh; the convection step is performed by considering discrete point vortices in a Lagrangian framework. For the simulation of high Reynolds number flows, a Large Eddy Simulation (LES) model is used to account for the effects of small scale turbulent structures in the wake.

At each time step the computed fluid forces are mapped to a structural dynamics representation of the pipe, being a finite element implementation of the Bernoulli-Euler bending beam equation. Pipe motion is permitted in both the in-line, x, and cross-flow, y, directions. The resulting motion of the pipe is accounted for in each fluid simulation plane by holding the body stationary and subjecting it to a local inflow velocity vector equal to the local relative velocity of the free stream flow with respect to the pipe, hence making use of the kinematic equivalence of the body-fixed and inertial frames of reference. The interested reader is referred to Willden (2003) for a complete explanation of the code.

For the simulations reported in this paper between 16 and 64 computation planes were used to discretise the fluid domain in the spanwise direction, whilst 60 finite elements were used to discretise the pipe's structural model in the same direction. The pipe was treated as pin-pin ended. The two-dimensional fluid domain commenced 25 diameters upstream and extended 50 diameters downstream of the pipe centre. It traversed a distance of 50 diameters in the cross-flow direction, yielding a blockage ratio of 2%. The unstructured mesh was composed of between 26861 and 58973 triangular elements.

3. SCOPE OF THE INVESTIGATION

In total six flow profiles have been simulated; these are presented graphically in figure 1 as a function of the non-dimensional vertical coordinate z/L. The uniform and linearly sheared profiles, shown in figures 1(a) and 1(b) respectively, are replicas of those tested experimentally by Trim et al. For these two cases, seven flow

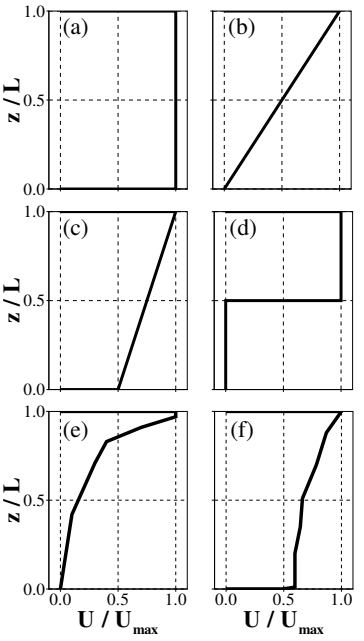

Figure 1: Flow profiles investigated. (a) uniform flow, (b) linearly sheared flow with $U/U_{max} = 0$ at $z/L = 0$, (c) linearly sheared flow with $U/U_{max} = 1/2$ at $z/L = 0$, (d) stepped flow, (e) typical Gulf of Mexico profile, (f) typical West of Shetland profile.

speeds have been simulated in the range 0.3 m/s $\leq U_{max} \leq$ 2.1 m/s, where U_{max} is the maximum flow speed and in all cases occurs at the free surface, $z = L$.

The remaining four flow profiles have been derived from numerous sources, and have been included as a theoretical exercise: there are no appropriate experimental data sets with which to draw direct quantitative comparisons. In each case four flow speeds were investigated in the range 0.3 m/s $\leq U_{max} \leq$ 1.2 m/s. The profile shown in figure 1(c) is a linearly sheared flow, in which $U/U_{max} = 1/2$ at $z = 0$, while figure 1(d) illustrates a stepped profile in which there is no current over the lower half of the pipe. The two remaining plots present generic profiles typical of flows in the Gulf of Mexico and West of Shetland regions (Petroluem and Natural Gas Industries (2005) and Fugro GEOS (2007) respectively) .

4. BENCHMARKING THE CODE

Before the investigation could begin in earnest, it was pertinent to benchmark the code over the appropriate Reynolds number range. The data sets of Gopalkrishnan (1993) and Staubli (1983) were chosen to provide the benchmarks. These pertain to experimental investigations of the prescribed transverse oscillations of circular cylinders at $Re = 10^4$ and $Re = 6 \times 10^4$ respectively. Both investigators varied the amplitude, A, and

frequency, f_o, of cylinder oscillation: Gopalkrishnan's investigation encompassed amplitudes $0.3 \leq A/D \leq 0.75$ and frequencies $0.05 \leq f_oD/U \leq 0.35$, whilst Staubli's investigation covered $0.1 \leq A/D \leq 0.8$ and $0.14 \leq f_oD/U \leq 0.18$. Simulations were performed to replicate these experiments. Comparison to the experimental data was made by considering six integral quantities; the oscillating component of the lift coefficient at the cylinder oscillation frequency, C_{Lo}, the phase angle by which the lift force led the cylinder displacement, ϕ_o, the components of the lift force in phase with the cylinder velocity and acceleration, C_{Lv} and C_{La} respectively, and the oscillating and mean drag coefficients, C_{Do} and C_{Dmean}.

The influence of three parameters on the agreement between the simulations and the experiments was investigated; the time step, δt, the characteristic dimension of the computational mesh, δx, and the sub-grid scale turbulence dissipation constant, C_s. It was found that C_s has a profound influence on the behaviour of the flow simulation. A value of $C_s = 1.7$ was found to provide optimal agreement in the integral quantities listed above. For a summary of the benchmarking results the interested reader is referred to McSherry et al (2007).

5. RISER RESPONSE

Figure 2 presents a comparison of various experimental and numerical response characteristics for the uniform flow profile case. Figures 2(a) and 2(b) reveal a good level of agreement in the spanwise mean and maximum of the temporal standard deviation of riser displacement, σ_{mean} and σ_{max} respectively, for both the in-line and cross-flow directions. It is however noted that there is a degree of scatter in the agreement of σ_{max}, which increases with flow speed, particularly in the cross-flow direction. The displacement-dominant mode numbers (figure 2(c)) are also found to be in good agreement, although the simulations did display a trend for over-predicting the response frequencies of the displacement-dominant modes at the higher flow speeds considered (figure 2(d)). The variations of the same quantities in the case of linearly sheared flow displayed similar trends to those observed in the uniform case, with reasonable overall agreement but some over-prediction of f_x^k and f_y^k, the repsonse frequencies of the in-line and cross-flow displacement-dominant modes, at high U_{max}.

Figure 3 presents a detailed account of the simulated pipe response for uniform flow at $U = 0.6\,\mathrm{m/s}$. From the axial variation of the pipe's response, figure 3(a), it is clear that the riser's cross-flow response is dominated by response in the 4^{th} mode. However, it is more difficult to ascertain the in-line displacement-dominant mode from this figure. Figure 3(c), the result of a modal analysis in which the riser displacement has been decomposed into linearized modes of vibration, shows that the displacement-dominant in-line modes are the 7^{th} and 8^{th}.

Figure 3(b) shows that the curvature of the model riser is dominated by higher modes than dominate its displacement. At this flow speed the 16^{th} mode is dominant with respect to curvature in the in-line direction, approximately double the mode number that is dominant with respect to displacement in the same direction. In the cross-flow direction the curvature is dominated by the 12^{th} mode; three times the displacement-dominant mode number in that direction.

The dashed contour lines in figure 3(c) represent curves of equal modal curvature contributions, which follow the relationship $\sigma_c^k \propto 1/k^2$, where σ_c^k is the standard deviation of the curvature of the k^{th} mode. The figure illustrates that, although relatively small amplitude oscillation may occur in a given high mode, that mode may still be dominant with respect to curvature. The figure shows that the 12^{th} cross-flow mode has a displacement amplitude of approximately one fifth of that of the displacement-dominant 4^{th} mode, but that the 12^{th} mode is still dominant with respect to curvature as its curvature contribution exceeds that of the 4^{th}. Likewise, the curvature contribution of the 16^{th} in-line mode is approximately double that of the displacement-dominant 7^{th} and 8^{th} in-line modes.

The variation of modal displacements depicted in figure 3(c) reveals a series of response envelopes in both the in-line and cross-flow directions, the peak modal response of which decrease with increasing mode number. Figure 3(d) shows that the modes corresponding to the cross-flow displacement peaks respond at the excitation frequency, $f_vD/U \approx 0.16$, and odd harmonics of it, with the 12^{th} mode responding at around $3f_vD/U$. Furthermore, the displacement-dominant in-line response occurs at around $2f_vD/U$, and a harmonic response in mode 16 occurs at around twice this frequency, i.e. $4f_vD/U$.

The high mode number curvature variations evidenced in figure 3(b) are the result of high curvature contributions from harmonically excited modes of vibration. This result has been observed in some, but not all, of the other flow cases that have been investigated. In some

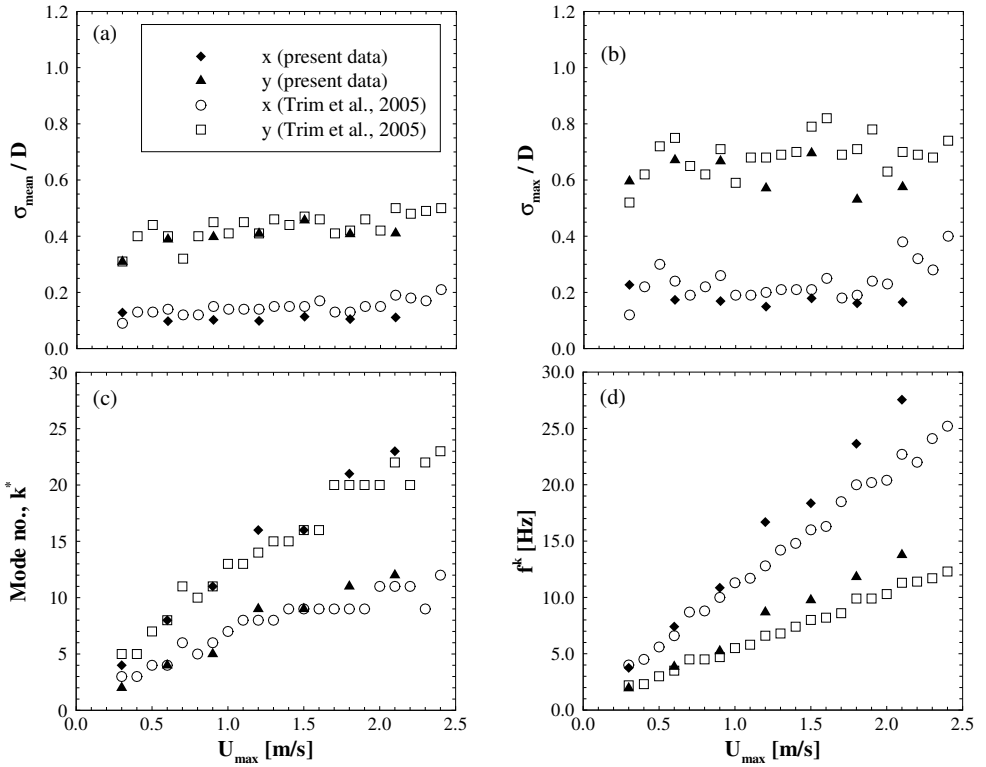

Figure 2: Simulated and observed riser response characteristics as a function of flow speed; uniform flow. (a) and (b) spatial (spanwise) mean, σ_{mean}/D, and maximum, σ_{max}/D, of the temporal standard deviation of riser response in the in-line, x, and cross-flow, y, directions, (c) and (d) displacement-dominant mode number, k^*, and its response frequency, f^k, in the in-line and cross-flow directions.

cases the displacement-dominant mode also dictates the extent of the riser's curvature in both the x and y directions, while in others perhaps σ_{cy} may be dominated by a harmonically excited mode while σ_{cx} remains dominated by the displacement-dominant mode, and vice-versa.

Figure 4 depicts the spanwise variations of the standard deviations of displacement and curvature in the x and y directions, for the six flow profiles introduced in figure 1, each with the same maximum (surface) flow speed, $U_{max} = 1.2$ m/s. In every case except the Gulf of Mexico profile (e), the variation of cross-flow curvature is seen to be dominated by a super-harmonically excited mode. In all super-harmonically dominated curvature cases the super-harmonic mode responds at three times the frequency of the displacement-dominant mode, hence yielding curvature dominant mode numbers of between 2.5 and 3 times the displacement-dominant mode number.

The propensity for super-harmonic responses to dominate in-line curvature is seen to be less than in the cross-flow direction, with only the second linearly sheared flow profile (c) and the (relatively similar) West of Shetland profile (f) being dominated in curvature by super-harmonic responses at twice the frequency of the in-line displacement-dominant mode. This is to be expected as the first in-line harmonic occurs at just twice the frequency of the principal in-line displacement, whilst the first cross-flow harmonic occurs at three times the frequency of the principal cross-flow displacement. Hence, to be dominant in curvature the first cross-flow harmonic must have an amplitude exceeding just 1/9 of that of the cross-flow displacement-dominant mode, whilst the first in-line harmonic requires an amplitude exceeding 1/4 of that of the in-line displacement-dominant mode. Hence, super-harmonic dominance of curvature is more prolific in cross-flow than in the in-line direction.

6. CONCLUSIONS

It has been shown that responses in high modes of vibration at harmonics of the displacement-dominant response frequency can be important with regard to the curvature variation along the riser. Furthermore, the results of the present study indicate that these higher harmonically excited modes of vibration can be influential not only in idealised flows, but also when the riser is subjected to more realistic flow profiles. These realistic flow profiles will be investigated in greater depth, with a larger range of flow speeds simulated, and the findings presented at the con-

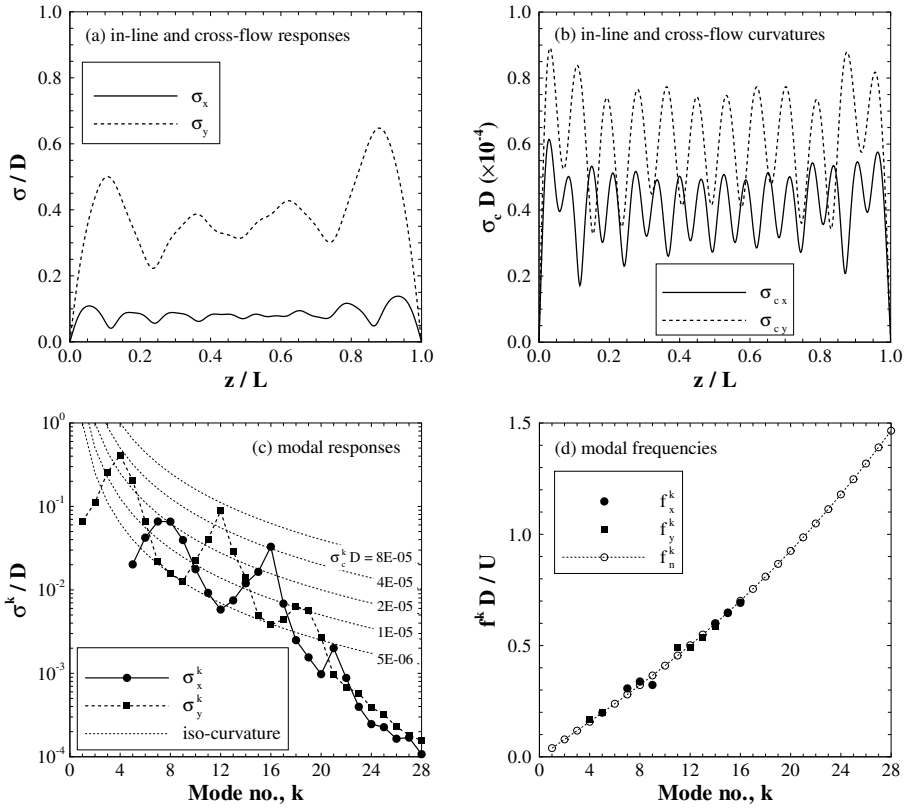

Figure 3: Simulated in-line, x, and cross-flow, y, riser response characteristics for uniform flow at $U_{max} = 0.6$ m/s. (a) and (b) spanwise variation, z/L, of the standard deviation of riser displacement, σ/D, and curvature, $\sigma_c D$, (c) standard deviation of modal displacements, σ^k/D, with iso-contours of modal curvature contributions, and (d) modal natural frequencies, $f_n^k D/U$, and response frequencies, $f^k D/U$, of modes with curvatures exceeding 25% of the curvature of the curvature-dominant mode.

ference. The implications of these higher harmonic responses on the fatigue damage rate will also be assessed and presented at the conference.

7. ACKNOWLEDGEMENTS

The authors would like to express their gratitude to the Engineering and Physical Sciences Research Council (UK), the Royal Academy of Engineering (UK) and BP Exploration Ltd., who have supported this work. The authors would also like to thank the Norwegian Deepwater Programme for some of the data used in this study.

8. REFERENCES

Gopalkrishnan, R., 1993, Vortex-induced forces on oscillating bluff cylinders. Ph.D thesis, Massachusets Institute of Technology, U.S.A.

McSherry, R.J., Willden, R.H.J., Graham, J.M.R, 2007, Numerical simulations of the flow past cross-flow oscillating circular cylinders and marine pipes. Proc. 26^{th} *Int. Conf. on Offshore Mechanics and Arctic Engineering, San Diego.*

Petroleum and Natural Gas Industries - Specific Requirements for Offshore Structures Part 1: Metocean Design and Operating Considerations, Table C23 and C24, 2005. ISO 19901-1:2005.

Staubli, T., 1983, Calculation of the vibration of an elastically mounted cylinder using experimental data from forced oscillation. In *Journal of Fluids Engineering* **105**: 225-229.

Toebes, G., 1969, The unsteady flow and wake near an oscillating cylinder. In *ASME Journal of Basic Engineering* **91**: 493-502.

Trim, A.D., Braaten, H., Lie, H., Tognarelli, M.A., 2005, Experimental investigation of vortex-induced vibration of long marine risers. In *Journal of Fluids and Structures* **21**: 335-361.

West of Shetland Current Criteria 2007, Fugro GEOS Reference No. C50470/4770/R1, 2008.

Willden, R.H.J., 2003, Numerical prediction of the vortex-induced vibrations of marine riser pipes. Ph.D thesis, University of London.

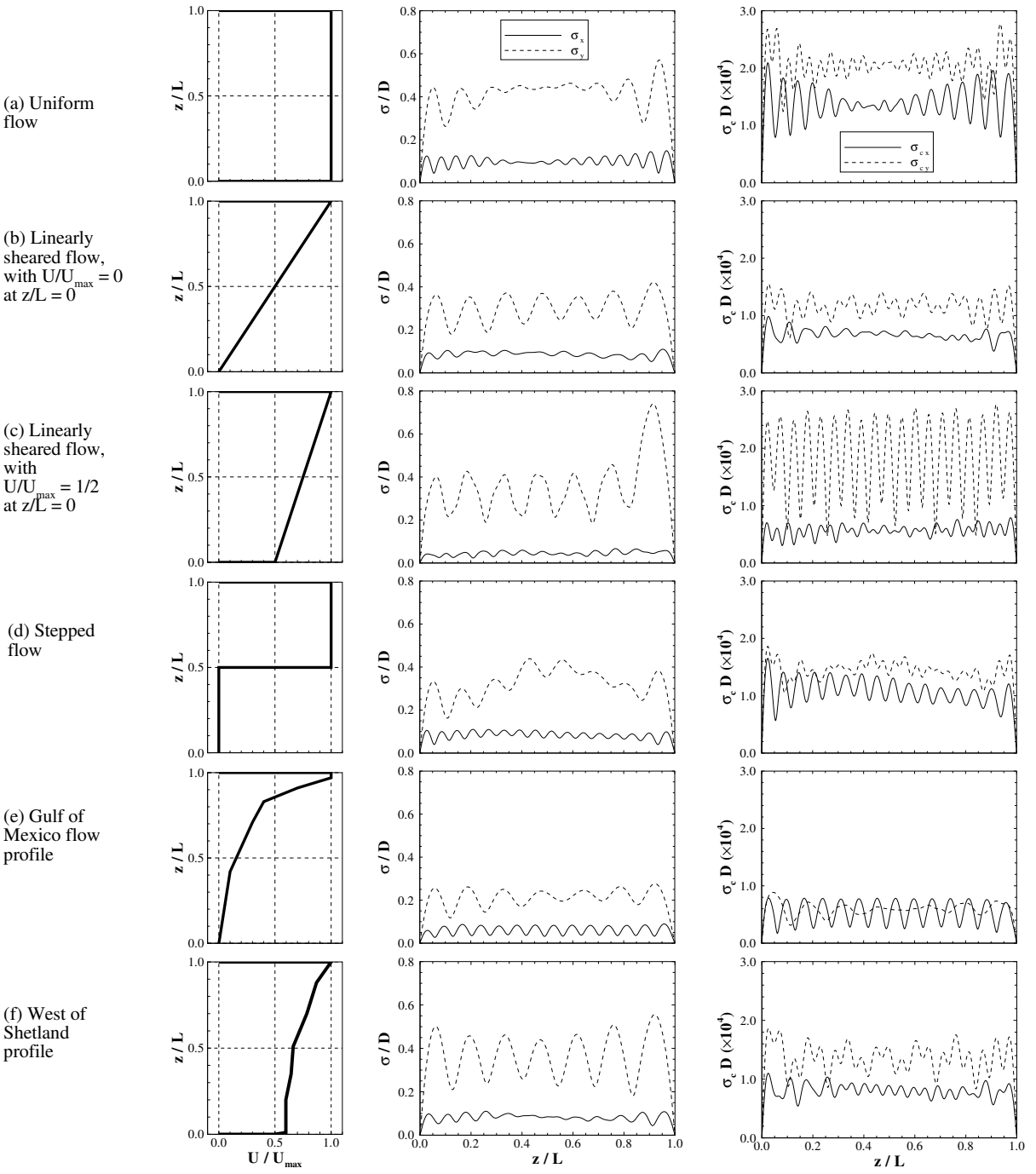

Figure 4: Influence of harmonic responses on pipe curvature. The plots present spanwise variations, z/L, of the temporal standard deviations of riser displacement (centre plots), σ/D, and curvature (right hand side), $\sigma_c D$, in the in-line, x, and cross-flow, y, directions, for the six flow profiles (left hand side). In all cases $U_{max} = 1.2$ m/s.